Electronic Supplementary Information

Co-Mo-P carbon nanosphere derived from metal-organic frameworks as high-performance catalyst towards efficient water splitting

Nan Li#, Yi Guan#, Yongliang Li*, Hongwei Mi, Libo Deng, Lingna Sun, Qianling Zhang, Chuanxin He, Xiangzhong Ren*

College of Chemistry and Environmental Engineering, Shenzhen University, Shenzhen, Guangdong 518060, P.R. China

Corresponding author:

Xiangzhong Ren, Email: renxz@szu.edu.cn, Tel/Fax: +86-755-26558134

Yongliang Li, Email: liyli@szu.edu.cn, Tel/Fax: +86-755-26536627

# These authors contributed equally to this work and should be considered co-first authors.

Chemicals

Molybdenum trioxide (MoO_3;≥99.0%), Imidazole ($C_3H_4N_2$; ≥99.0% Zinc acetate ($Zn(Ac)_2$; ≥99.0%), Cobalt acetate ($Co(Ac)_2$; ≥99.0%), 2-methylimidazole (2-mIm; 98.0%), Ammonium hydroxide ($NH_3 \cdot H_2O$, 25-28wt.%), ethanol (EtOH, absolute), All the chemicals were purchased from Aladdin Industrial Corporation. and used as received without further purification.

Synthesis of Mo-MOF

Mo-MOF was modified according to the preparation process previously reported [28]. Firstly, 0.068 g of imidazole and 0.144 g of MoO_3 were mixed in 100 mL specific solvent (the composition of the solution is methanol and water in a volume ratio of 3:2). Then after stirred for 12 hours, the product has been centrifuged three times at 10000 rpm to obtain a precipitate. Finally, the products have been dispersed in 30 mL of ammonia (AR, 25%-28%),

Synthesis of Co/Co_3O_4/Mo-MOF

In a typical procedure, 8 mL of 0.2 mol L^{-1} cobalt nitrate solution was gradually added dropwise to Mo-MOF ammonia aqueous solution, and stirred vigorously for 30 minutes. Then above solution was packed in a 100 mL Teflon autoclave, then put it at 180 °C for 4 hours. Then, resulting products was collected by centrifugation at 10000 rpm for 5 min and washed with ultrapure water until the pH is approximately equal to 7, and then place it in a 60℃ vacuum oven to dry overnight.

Synthesis of $Co/Co_3O_4/MoO_3$@NCNS products

The as-prepared Co/Co_3O_4/Mo-MOF was pyrolyzed at 400 °C with 10 °C min^{-1} rate in an Nitrogen atmosphere for 3 h, and then heated to 500/600/700 °C with the same heating rate, and kept for 4 h. The final product is $Co/Co_3O_4/MoO_3$@NCNS-500/600/700, respectively.

Synthesis of Co-Mo-P@NCNS products

Typically, 50 mg of $Co/Co_3O_4/MoO_3$@NCNS powders and 1 g of sodium hypophosphite are placed in the same quartz boat, and the latter is placed upstream side. Through the 300 °C pyrolysis process with a rate of 2 °C min^{-1} in Nitrogen atmosphere for 2 h, we can obtain phosphating products. The obtained phosphating product was then washed in 2M HCl for 3 h to eliminate accessible cobalt species on surface, then washed it with ethanol and deionized water several times and dry overnight in vacuum oven yielding the final product Co-Mo-P@NCNS-500/600/700.

Preparation of the Working Electrode

The electrocatalyst ink was prepared by dispersing 5 mg of samples in a mixture of 1.5 mL of ethanol and 40 μL of dilute aqueous Nafion solution (5 wt%). The working electrode was obtained by ultrasonically dispersing and dropping 15 μL of catalyst ink on a glassy carbon RRDE (with a disk diameter of 4 mm, A_{disk}= 0.126 cm^2; inner/outer-ring diameter: 5.0/7.0 mm, A_{ring} = 0.188 cm^2) from BAS Inc. The electrocatalyst loading was 0.398 mg cm^{-2} based on the geometric electrode area of 0.126 cm^2.

Materials characterization

The crystallite structure was investigated by X-ray diffraction (XRD) on a PANalytical/Empyrean diffractometer with CuKα radiation. The morphology and microstructure were inspected using a field emission scanning electron microscope (FESEM, JEOL JSM-7800F) and transmission electron microscopy (TEM, JEOL-F200), respectively. X-ray photoelectron spectroscopy (XPS) measurements were performed on a K-Alpha+ spectrometer using a monochromic Al X-ray source. Raman spectra were obtained using a Renishaw/Invia Reflex spectrometer coupled with a 633 nm laser. Nitrogen adsorption-desorption isotherms were measured using a BELSORP-max instrument. The specific surface area and pore size distribution were determined using the Brunauer-Emmett-Teller (BET) theory and the nonlocal density functional theory (NLDFT) method, respectively.

Electrochemical tests

All the measurements were carried out on a CHI760E electrochemical workstation (CHInstruments, Inc., Shanghai) with a MSR electrode rotator (BAS RRDE-3A,

Japan). The three-electrode cell was used to perform the electrochemical measurements, with an Ag/AgCl (3M KCl) and graphite rod serving as the reference electrode and counter electrode, respectively. The HER and OER performance was evaluated in N_2-saturated 1 M KOH solutions. The potential was converted to a potential versus reversible hydrogen electrode (RHE) according to $E_{(vs.RHE)} = E_{(vs. Ag/AgCl)}+0.222+0.059pH$. The OER/HER polarization curves were measure at 25℃ with a scan rate of 5 mV s^{-1}, and the rotation speed is controlled at 1600 rpm. The i-t chronoamperometric response was used to evaluate the long-term durability, which was conducted at a rotation rate of 1600 rpm for 85000s.

Computational Method

All the density functional theory (DFT) calculations were performed by Vienna Ab-initio Simulation Package[1, 2] (VASP), employing the Projected Augmented Wave[3] (PAW) method. The revised Perdew-Burke-Ernzerhof (RPBE) functional was used to describe the exchange and correlation effects.[4-6]. For all the geometry optimizations, the cutoff energy was set to be 450 eV. A 3×3×1 Monkhorst-Pack grids[7] was used to carry out the surface calculations on MoP and MoP@Co. The MoP@Co structure was modelled as one Co_4 cluster on the (101) surface of MoP. At least 20 Å vacuum layer was applied in z-direction of the slab models, preventing the vertical interactions between slabs.

In alkaline conditions, OER could occur in the following four elementary steps:

$OH^- + * \rightarrow *OH + e^-$

$*OH + OH^- \rightarrow *O + H_2O + e^-$

$*O + OH^- \rightarrow *OOH + e^-$

$*OOH + OH^- \rightarrow * + O_2 + H_2O + e^-$

where * denotes the active sites on the catalyst surface. Based on the above mechanism, the free energy of three intermediate states, *OH, *O, and *OOH, are important to identify a given material's OER and ORR activity. Meanwhile, HER in alkaline condition occurs via the following elementary steps:

$H_2O + * \rightarrow *H\text{-}OH$

$*H \rightarrow ½\ H_2 + *$

In this mechanism, water dissociated into an adsorbed H-OH state at the catalyst surface, making *H-OH the first reaction intermediate. Thereafter, the adsorbed OH dissolved into the solution, and the adsorbed H combine with an electron and proton pair to form the gaseous hydrogen molecule.

The computational hydrogen electrode (CHE) model[8] was used to calculate the free energies of OER and HER, based on which the free energy of an adsorbed species is defined as

$$\Delta G_{ads} = \Delta E_{ads} + \Delta E_{ZPE} - T\Delta S_{ads}$$

where ΔE_{ads} is the electronic adsorption energy, ΔE_{ZPE} is the zero point energy difference between adsorbed and gaseous species, and $T\Delta S_{ads}$ is the corresponding entropy difference between these two states. The electronic binding energy is referenced as $½\ H_2$ for each H atom, and ($H_2O - H_2$) for each O atom, plus the energy of the clean slab. The corrections of zero-point energy and entropy of the OER and HER intermediates can be found in the supporting information.

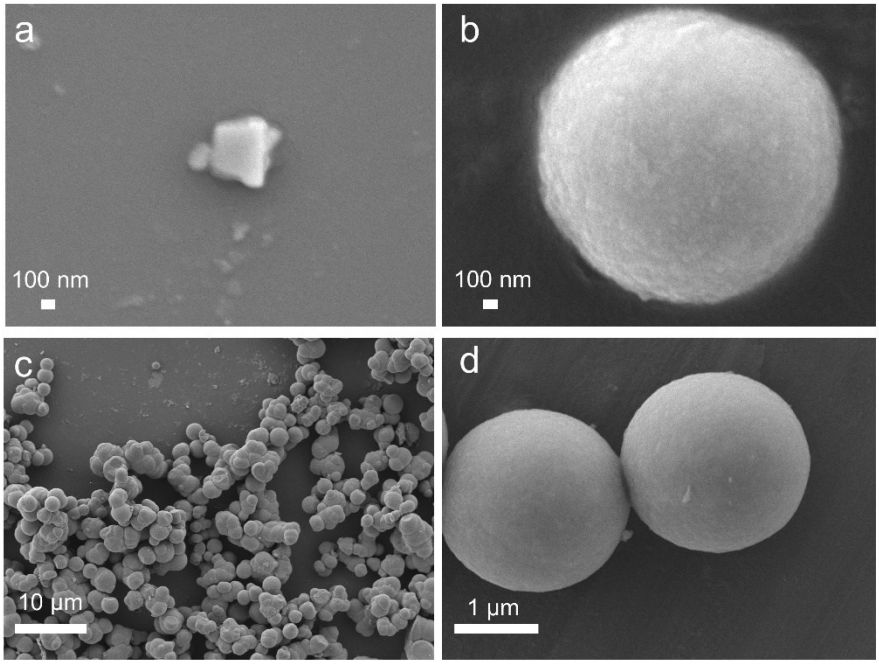

Figure S1. SEM images of (a) customized Mo-MOFs and (b) Co/Co_3O_4/Mo-MOF; (c) and (d) Co-Mo-P@NCNS-600.

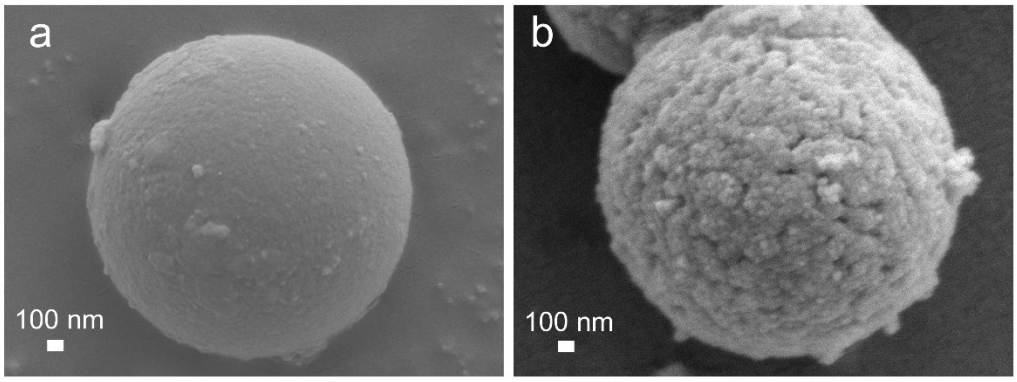

Figure S2. SEM images of (a) Co-Mo-P@NCNS-500 and (b) Co-Mo-P@NCNS-700.

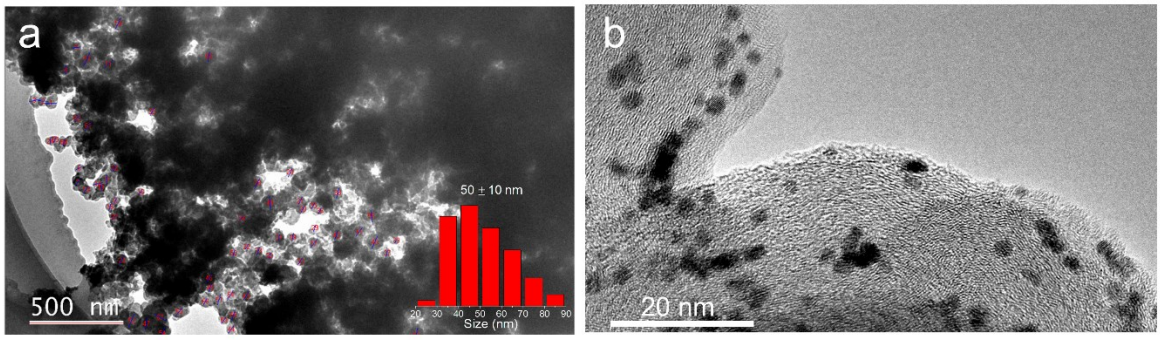

Figure S3. (a, b) HRTEM images of Co-Mo-P@NCNS-600.

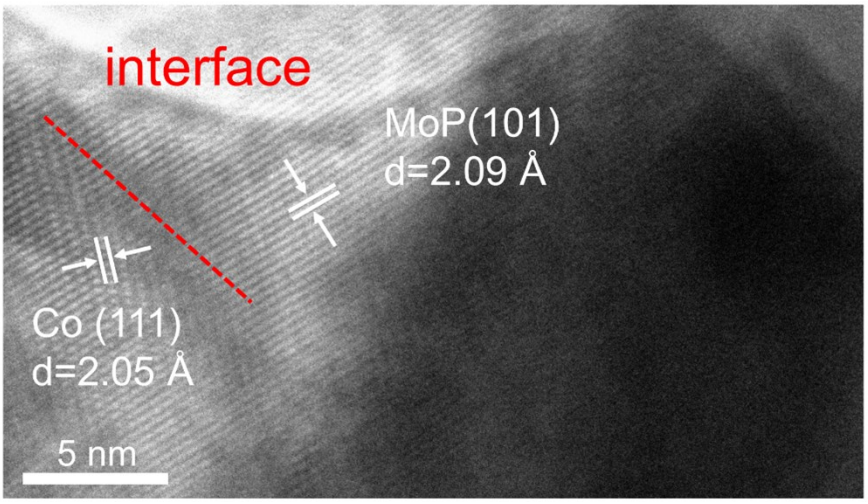

Figure S4. HRTEM of Co-Mo-P@NCNS-600, which demonstrate the obvious interface between Co(111) fact and MoP(101).

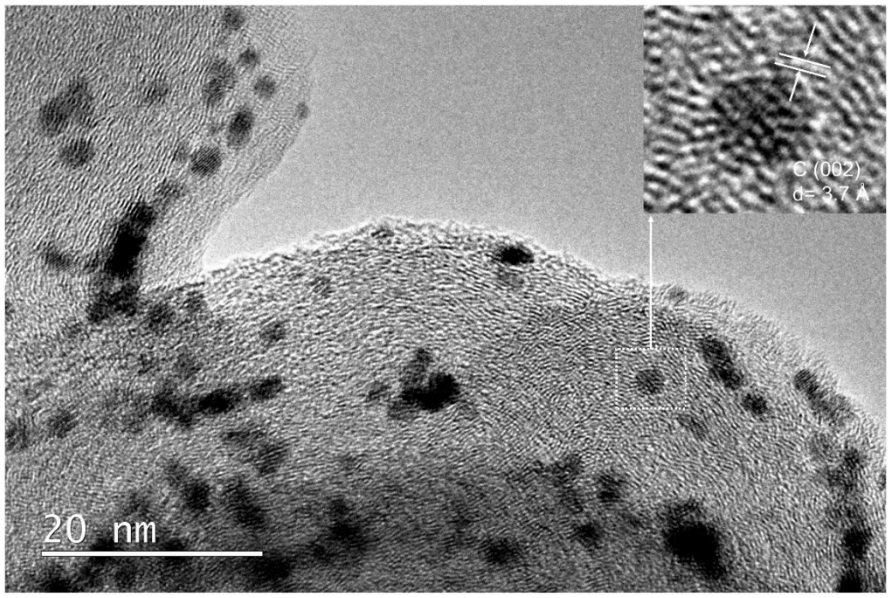

Figure S5. The HRTEM image of Co-Mo-P @NCNS-600.

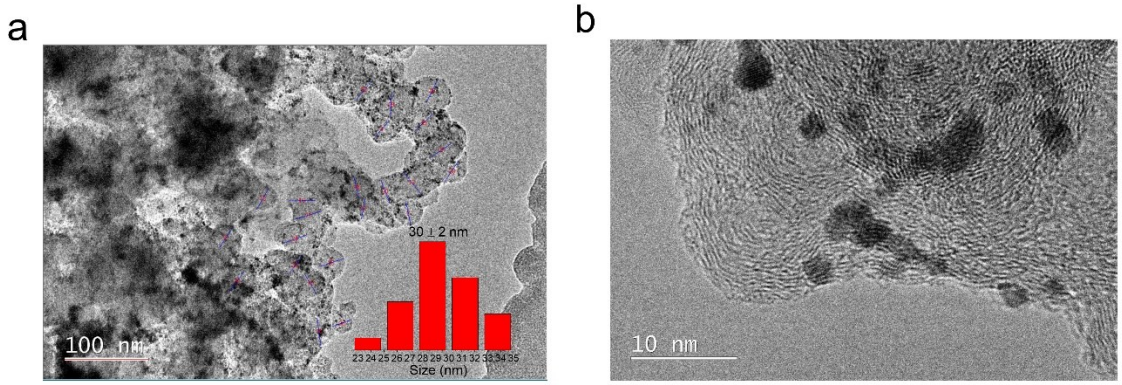

Figure S6. The HRTEM image of Co-Mo-P @NCNS-500.

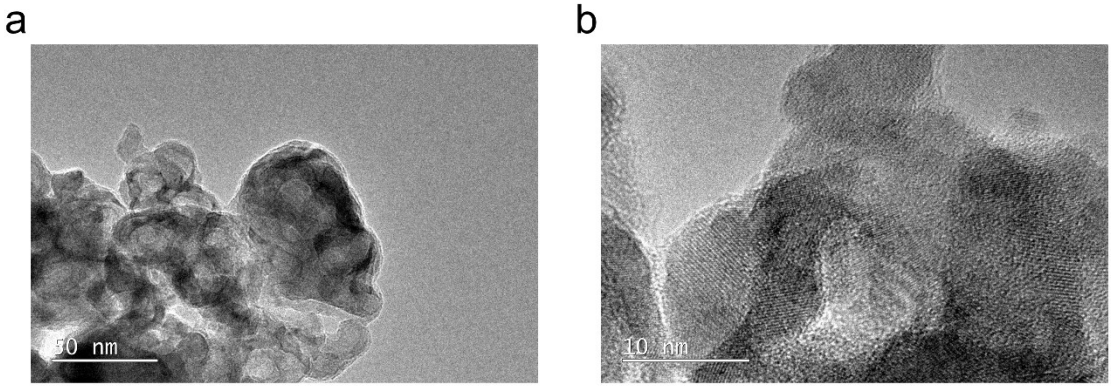

Figure S7. The HRTEM image of Co-Mo-P @NCNS-700.

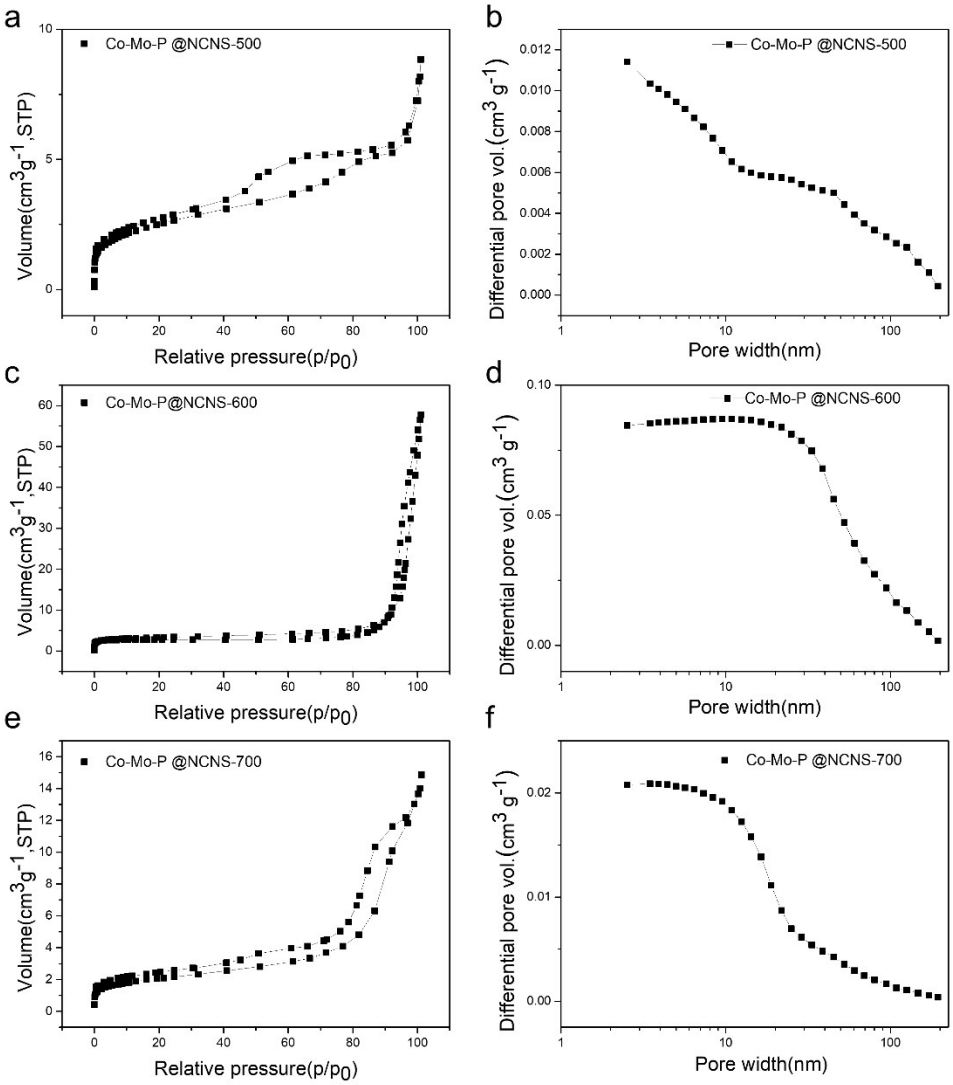

Figure S8. Specific surface area and pore size for (a, b) Co-Mo-P @NCNS-500 and (c, d) Co-Mo-P @NCNS-600 and (e, f) Co-Mo-P @NCNS-700.

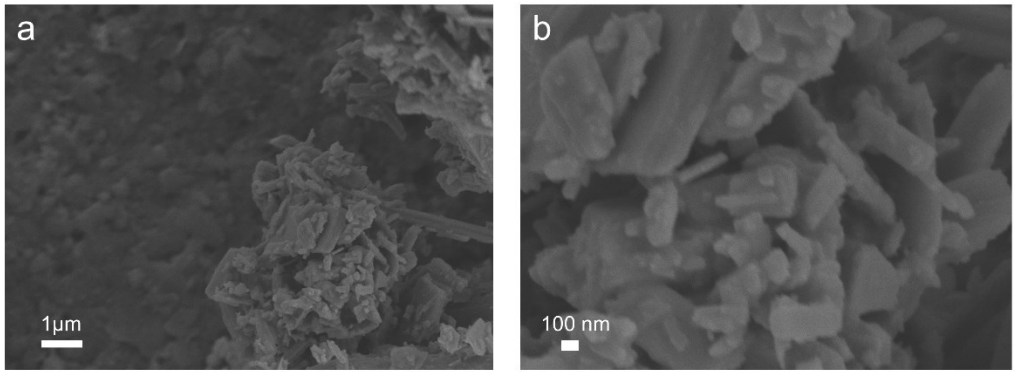

Figure S9. SEM images of MoP@NCNS-600.

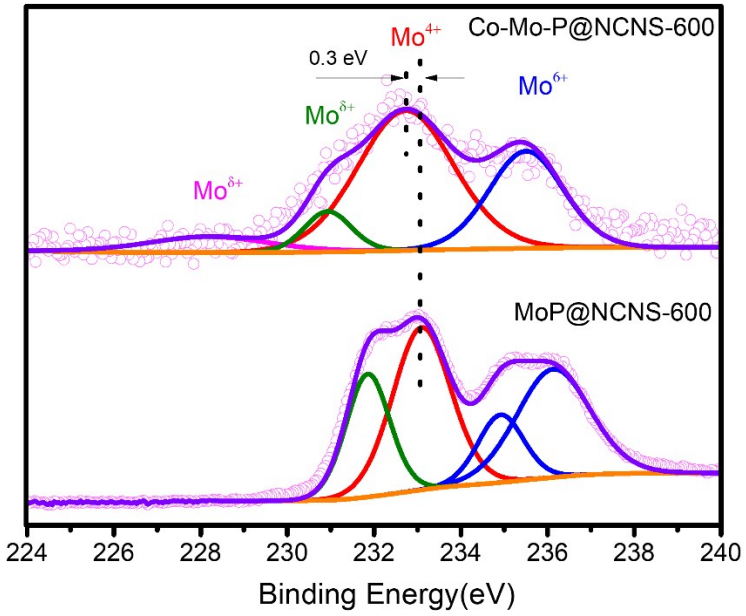

Figure S10. Mo 3d XPS spectra of Co-Mo-P@NCNS-600 and MoP@NCNS-600.

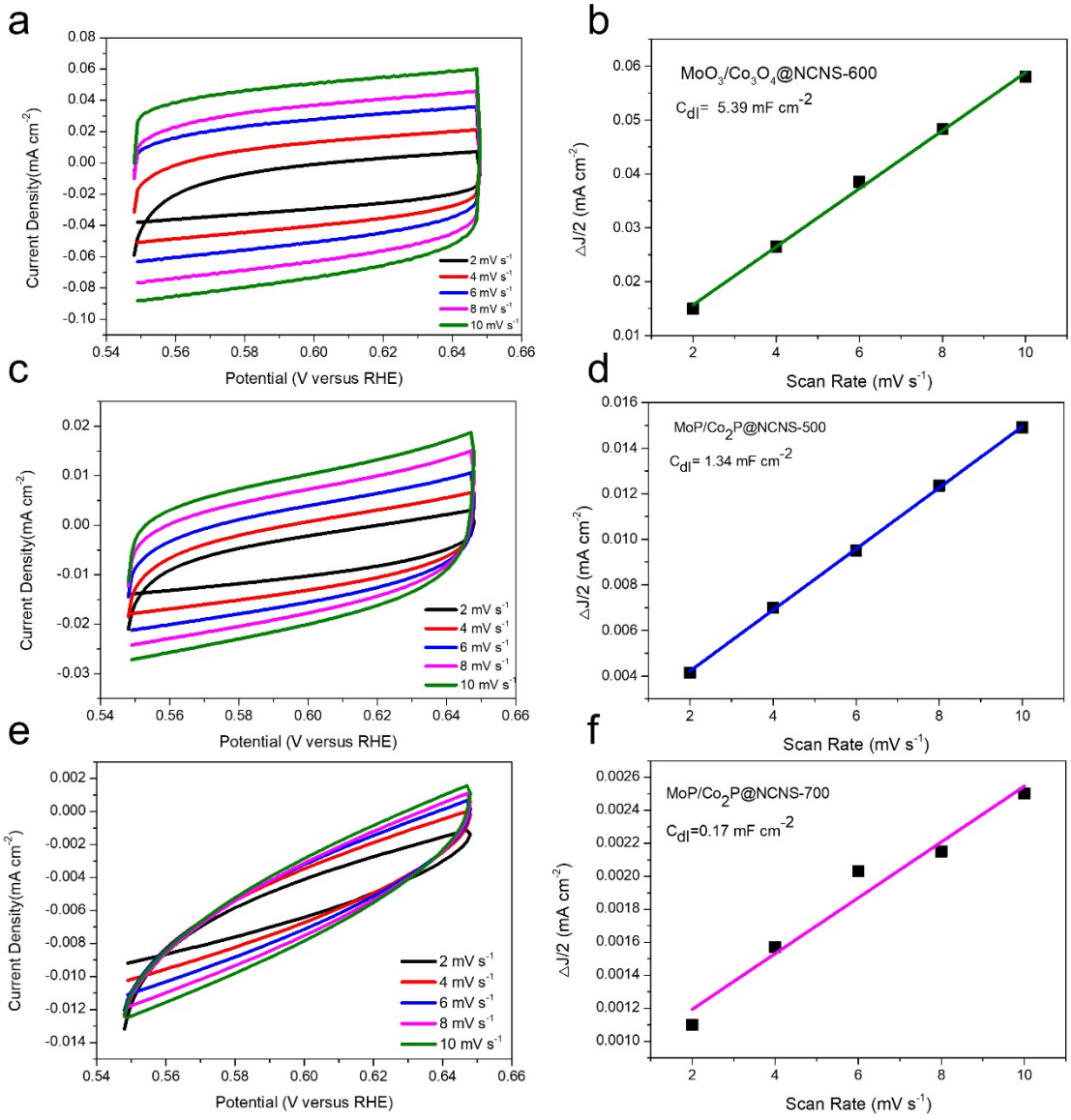

Figure S11. Cyclic voltammograms in the region of 0.548-0.648 V vs. RHE at various scan rates and the corresponding linear fitting of the capacitive currents vs. scan rates to estimate the C_{dl}. (a, b) for $Co/Co_3O_4/MoO_3$@NCNS-600@NCNS-600; (c, d) for Co-Mo-P @NCNS-500 and (e, f) Co-Mo-P @NCNS-700.

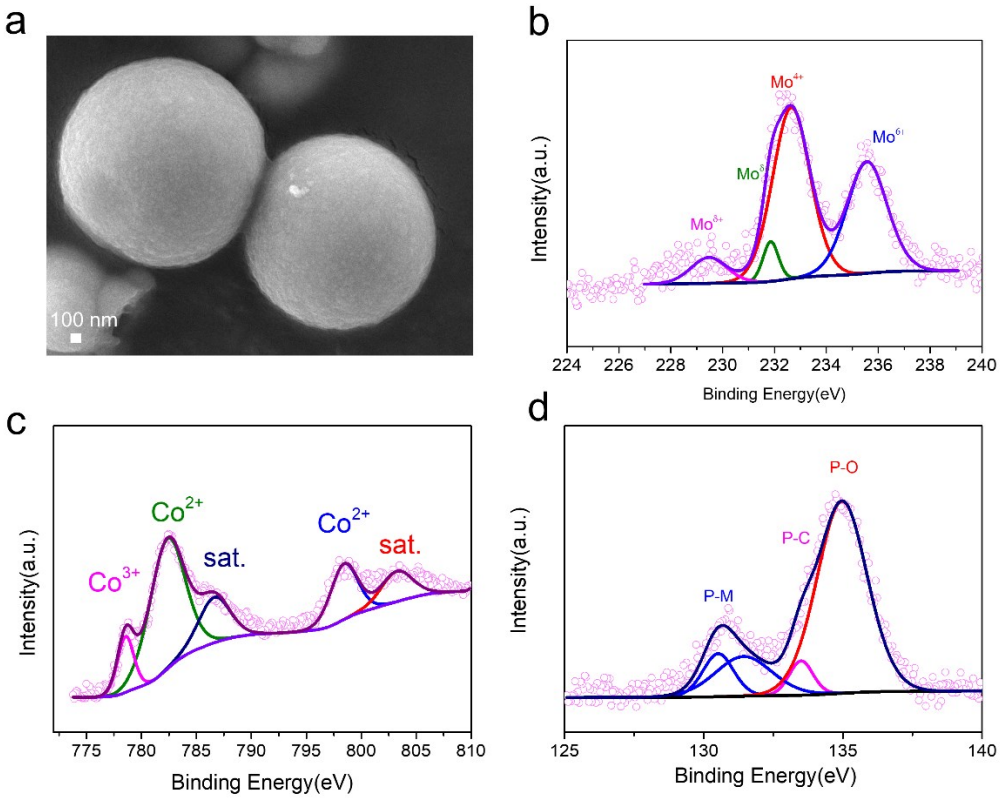

Figure S12. (a) SEM image and (b,c,d) XPS spectra of Co-Mo-P@NCNS-600 after HER test.

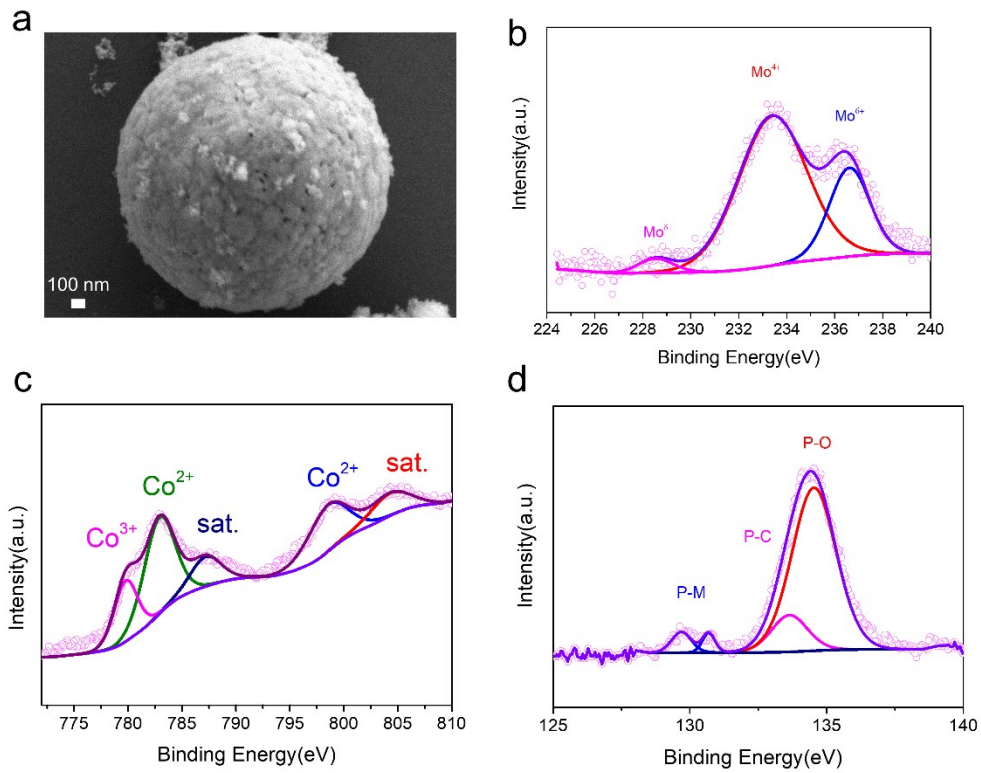

Figure S13. (a) SEM image and (b,c,d) XPS spectra of Co-Mo-P@NCNS-600 after OER test.

Figure S14. Optical photographs of overall water splitting using Co-Mo-P@NCNS-600 as both cathode and anode.

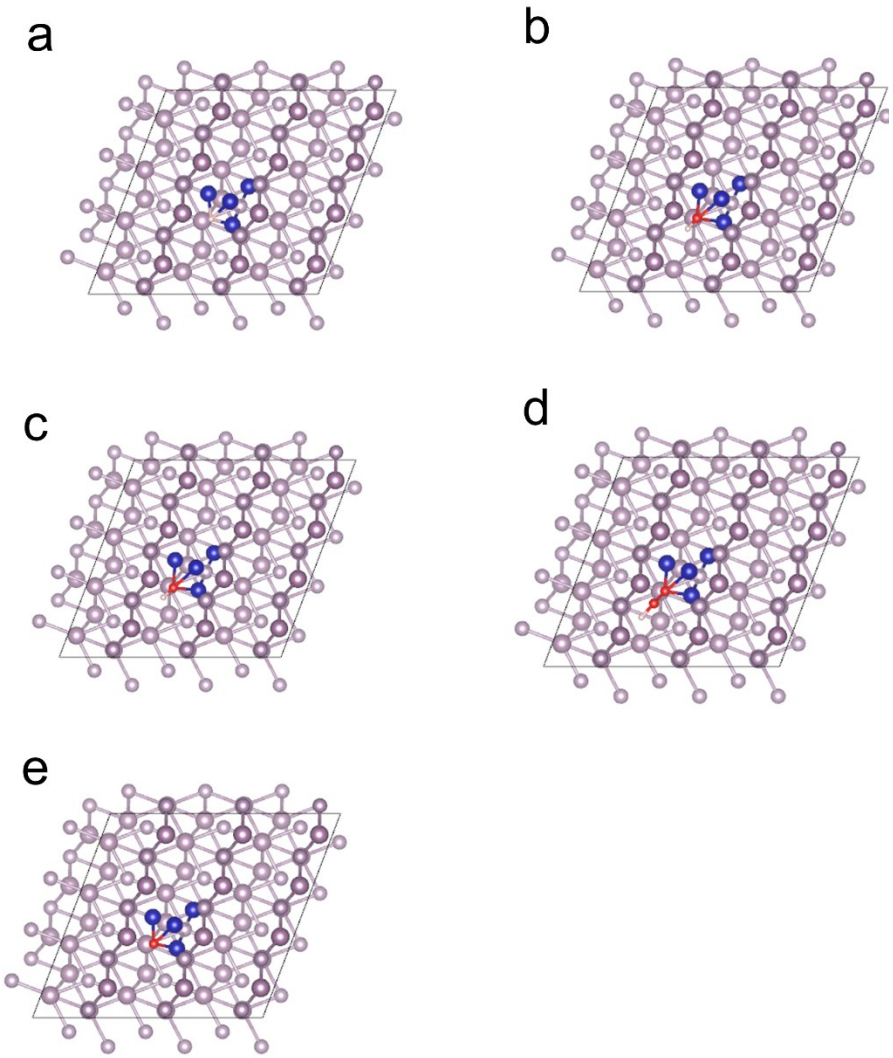

Figure S15. Simulation modul of (a) Co-Mo-P@NCNS-600--H, (b) Co-Mo-P@NCNS-600 ---HandOH and (c) Co-Mo-P@NCNS-600 ---O;(d) Co-Mo-P@NCNS-600 ---OH, (e) MoO_2—OH and (f) Co-Mo-P@NCNS-600—OOH.

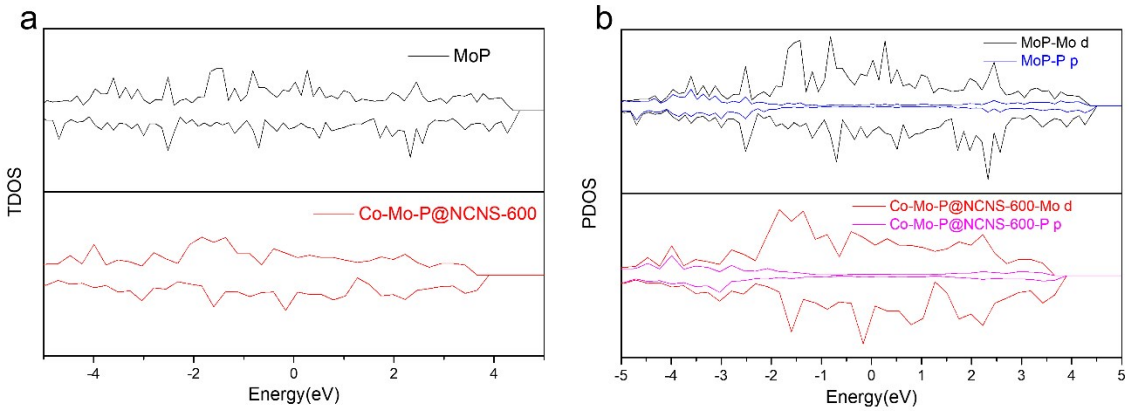

Figure S16. (a) TDOS and (b) PDOS of Co-Mo-P@NCNS-600 and pure MoP.

Table S1. Activities for HER of Co-Mo-P@NCNS-600 catalysts and other reported phosphide-based electrocatalysts

Literature	Catalyst	Electrolyte	Substrate	η_{10} (mV *vs.* RHE)
This work	Co-Mo-P@NCNS-600	1 M KOH	GCE	62
Applied Catalysis B: Environmental, 2019, 245, 528, 535.	CoP/MoP@NC	1 M KOH	Carbon cloth	94
Energy Environ. Sci. 11 (2018) 872-880.	Ni-Co-P HNBs	1 M KOH	Ni foam	107
Angew. Chem. Int. Ed. 58 (2019) 4923-4928	Co/β-Mo_2C@N-CNTs/GCE	1 M KOH	GCE	170
Adv. Funct. Mater. 28 (2018) 1706847	NiFe LDH@NiCoP	1 M KOH	Ni foam	120
Adv. Funct. Mater. 27 (2017) 1703455.	Co_4Ni_1P	1 M KOH	RDE	129
Adv. Energy Mater. 8 (2018) 1703290	O-$Ni_{0.75}Fe_{0.25}P2$	1 M KOH	Carbon fibers	169

Nano Energy 39 (2017) 626-638.	3D-CNTA/NF	1 M KOH	Ni foam	185

Table S2. Activities for OER of MoP/Co_2P @NCNS -600 catalysts and other reported phosphide-based electrocatalysts

Literature	Catalyst	Electrolyte	Substrate	η_{10} (mV *vs.* RHE)
This work	Co-Mo-P@NCNS-600	1 M KOH	GCE	270
Applied Catalysis B: Environmental, 2019, 245, 528, 535.	CoP/MoP@NC	1 M KOH	Carbon cloth	270
Adv. Funct. Mater. 27 (2017) 1703455.	Co_4Ni_1P	1 M KOH	RDE	280
Nano Lett. 16 (2016) 7718-7725.	NiCoP	1 M KOH	Ni foam	280
Nano Energy 39 (2017) 626-638.	3D-CNTA/NF	1 M KOH	Ni foam	360
Adv. Energy Mater. 8 (2018) 1703290	O-$Ni_{0.75}Fe_{0.25}P_2$	1 M KOH	Carbon fibers	320
Angew. Chem. Int. Ed. 129 (2017) 3955-3958.	NiCoP/C	1 M KOH	RDE	330
Adv. Funct. Mater. 28 (2018) 1801136.	Co/NBC-900	1 M KOH	GCE	302
Nano Energy 48 (2018) 284-291.	$NiCo_2P_2$/GOD	1 M KOH	Ti	340

Table S3. A survey of the performance of overall water splitting with various

electrocatalysts

Literature	Catalyst	Substrate	Current density (mA cm^{-2})	Cell voltage (V)
This work	Co-Mo-P@NCNS-600	GCE	10	1.58
Applied Catalysis B: Environmental, 2019, 245, 528, 535.	CoP/MoP@NC	Carbon cloth	50	1.71
Angew. Chem. Int. Ed. 58 (2019) 4923-4928.	Co/β-Mo_2C@N-CNTs	GCE	10	1.64
Nano Energy 39 (2017) 626-638.	3D-CNTA	Ni foam	10	1.68
Adv. Energy Mater. 7 (2017) 1601555.	$Cu_{0.3}Co_{2.7}P$/NC	Ni foam	70	1.74
Nano Energy 34 (2017) 472-480.	$Ni_{1.5}Fe_{0.5}P$	Carbon fiber	20	1.635
Energy Environ. Sci. 11 (2018) 872-880.	Ni-Co-P HNBs	Ni foam	10	1.62
Applied Catalysis B: Environmental, 271 (2020) 118939.	Co@CNT	Ni foam	10	1.58

Table S4. The correction of zero point energy and entropy of the adsorbed and

gaseous species.

	ZPE(eV)	TS(eV)
*OOH	0.35	0
*O	0.05	0
*H	0.16	0.01
*OH	0.31	0.01
H_2O	0.56	0.67
H_2	0.27	0.41

[1] G. Kresse, J. Furthmüller, Efficient iterative schemes for ab initio total-energy calculations using a plane-wave basis set, Physical Review B, 54 (1996) 11169-11186

[2] G. Kresse, J. Hafner, Ab initio, Physical Review B, 49 (1994) 14251-14269

[3] P.E. Blöchl, Projector augmented-wave method, Physical Review B, 50 (1994) 17953-17979

[4] J.P. Perdew, K. Burke, M. Ernzerhof, Generalized Gradient Approximation Made Simple, Physical Review Letters, 77 (1996) 3865-3868

[5] Y. Zhang, W. Yang, Comment on ``Generalized Gradient Approximation Made Simple", Physical Review Letters, 80 (1998) 890-890

[6] B. Hammer, L.B. Hansen, J.K. Nørskov, Improved adsorption energetics within density-functional theory using revised Perdew-Burke-Ernzerhof functionals, Physical Review B, 59 (1999) 7413-7421

[7] H.J. Monkhorst, J.D. Pack, Special points for Brillouin-zone integrations, Physical review B, 13 (1976) 5188

[8] J.K. Nørskov, J. Rossmeisl, A. Logadottir, L. Lindqvist, J.R. Kitchin, T. Bligaard,

H. Jonsson, Origin of the overpotential for oxygen reduction at a fuel-cell cathode, The Journal of Physical Chemistry B, 108 (2004) 17886-17892